

Supporting Information

Carbon quantum dots bridged TiO₂/CdIn₂S₄ toward photocatalytic upgrading of polycyclic aromatic hydrocarbons to benzaldehyde

Jiangwei Zhang^{12#}, Fei Yu^{1#}, Xi Ke³, He Yu¹, Peiyuan Guo¹, Lei Du², Menglong Zhang^{1*} and Dongxiang Luo^{2*}

¹Institute of hydrogen energy for carbon peaking and carbon neutralization, School of Semiconductor Science and Technology, South China Normal University, Foshan, 528225, P.R. China

²School of Chemistry and Chemical Engineering/Huangpu Hydrogen Innovation Center, Guangzhou University, Guangzhou 510006, PR China

³Great Bay Area Branch of Aerospace Information Research Institute, Chinese Academy of Sciences, Guangzhou 510530, China

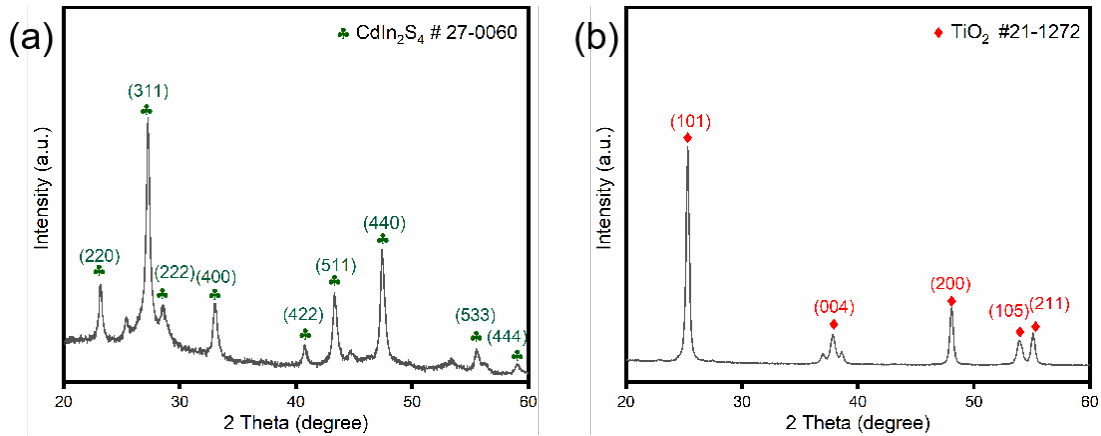


Figure S1: XRD of (a) bare CdIn₂S₄ and (b) bare TiO₂

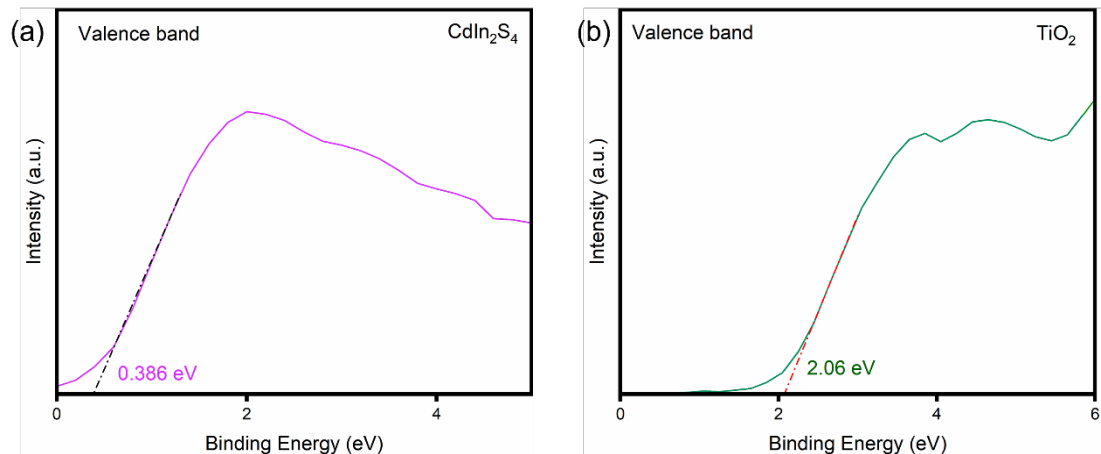


Figure S2: The valance band edges of (a) CdIn₂S₄ and (b) TiO₂.

After obtaining XPS valence band data, the following two formulas shall be used to convert the data into NHE[1] and RHE[2], respectively:

$$E_{VB,NHE} = \varphi + E_{VB,XPS} - 4.44 \quad (1)$$

$$E_{NHE} = E_{NHE} + 0.0591PH \quad (2)$$

where the φ represent work function of the instrument (4.2 eV).

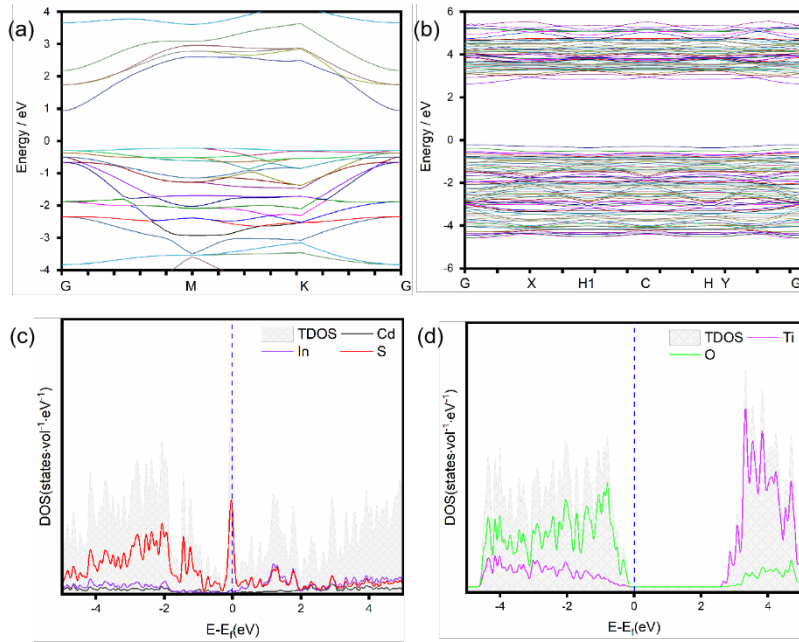


Figure S3: (a-b) the band structure of bare CdIn_2S_4 bulk and bare TiO_2 bulk, (c-d) the density of states for bare CdIn_2S_4 bulk and bare TiO_2 bulk

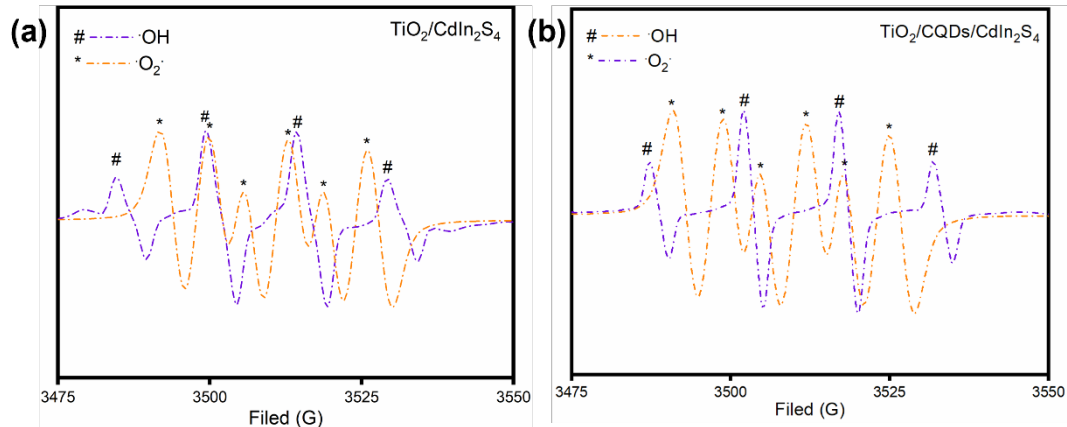


Figure S4: EPR spectrum of (a) $\text{TiO}_2/\text{CdIn}_2\text{S}_4$ and (b) $\text{TiO}_2/\text{CQDs}/\text{CdIn}_2\text{S}_4$.

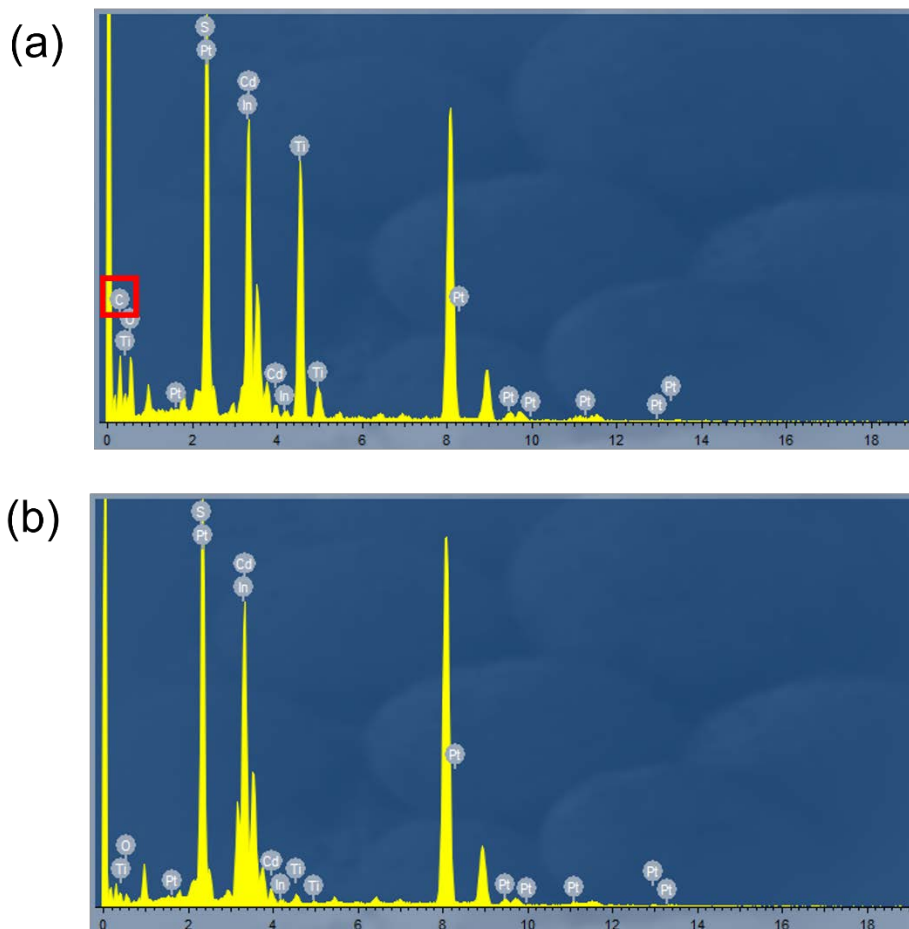


Figure S5: The elemental composition of (a) $\text{TiO}_2/\text{CQDs}/\text{CdIn}_2\text{S}_4$ and (b) $\text{TiO}_2/\text{CdIn}_2\text{S}_4$ analyzed by TEM-EDS.

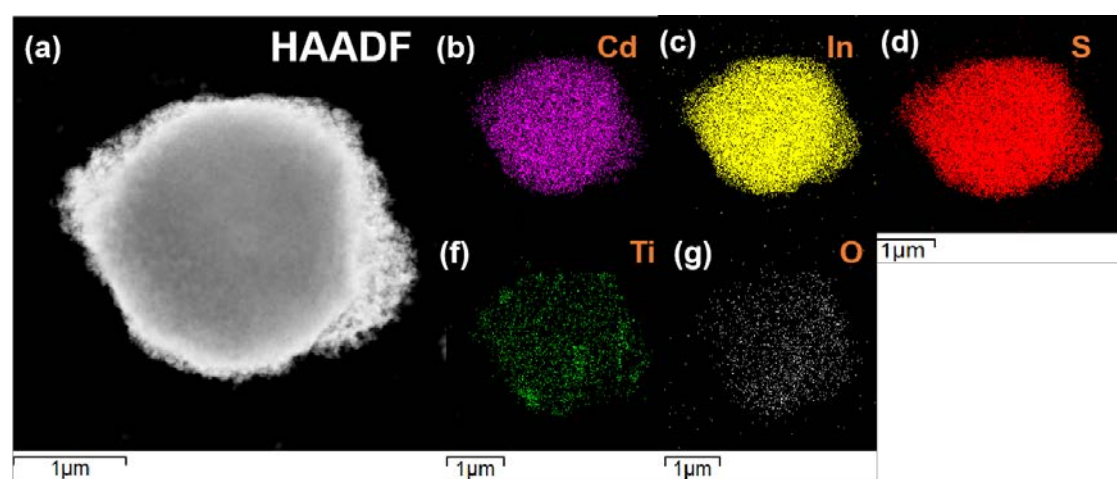


Figure S6: (a) HAADF TEM image of $\text{TiO}_2/\text{CdIn}_2\text{S}_4$ heterostructure, (b-g) respective elemental mapping of Cd, In, S, Ti and O.

Table S1. Relative atomic content of $\text{TiO}_2/\text{CQDs}/\text{CdIn}_2\text{S}_4$ and $\text{TiO}_2/\text{CdIn}_2\text{S}_4$.

Sample	C/%	Cd/%	In/%	S/%	Ti/%	O/%	Pt/%
$\text{TiO}_2/\text{CQDs}/\text{CdIn}_2\text{S}_4$	19.27	2.32	20.75	28.98	17.95	10.05	0.69
$\text{TiO}_2/\text{CdIn}_2\text{S}_4$	0	11.74	32.44	51.93	0.91	1.99	0.99

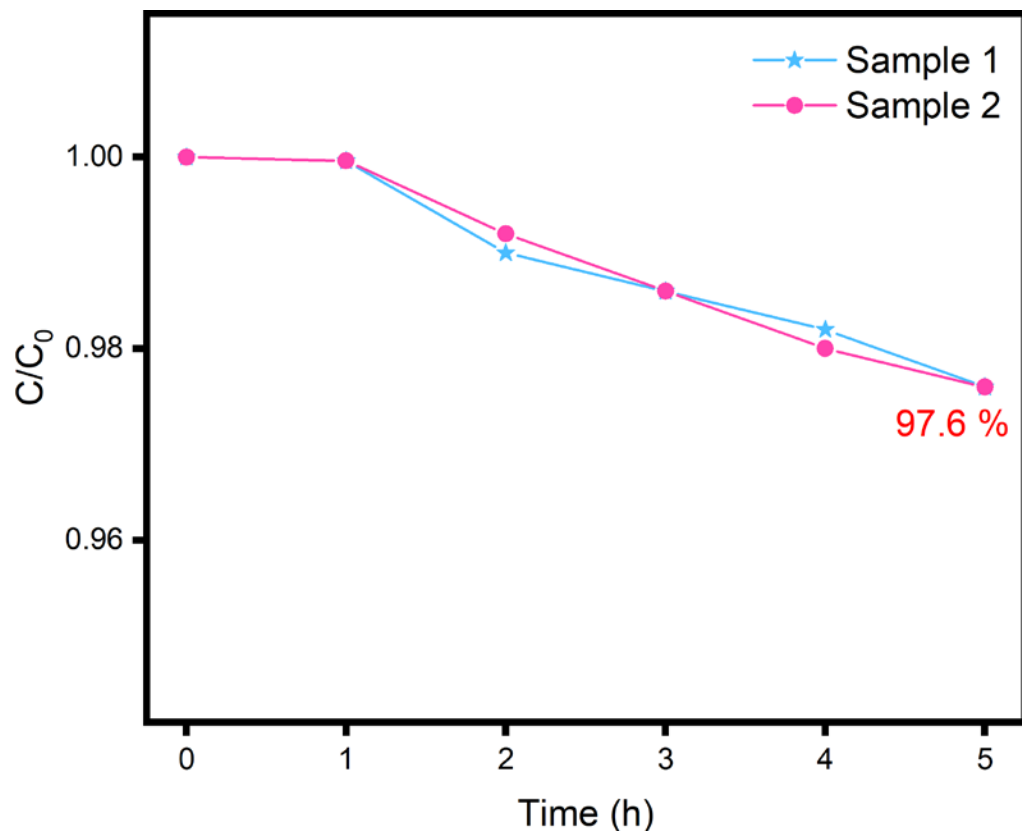


Figure S7: Stability of PAHs degradation of $\text{TiO}_2/\text{CQDs}/\text{CdIn}_2\text{S}_4$.

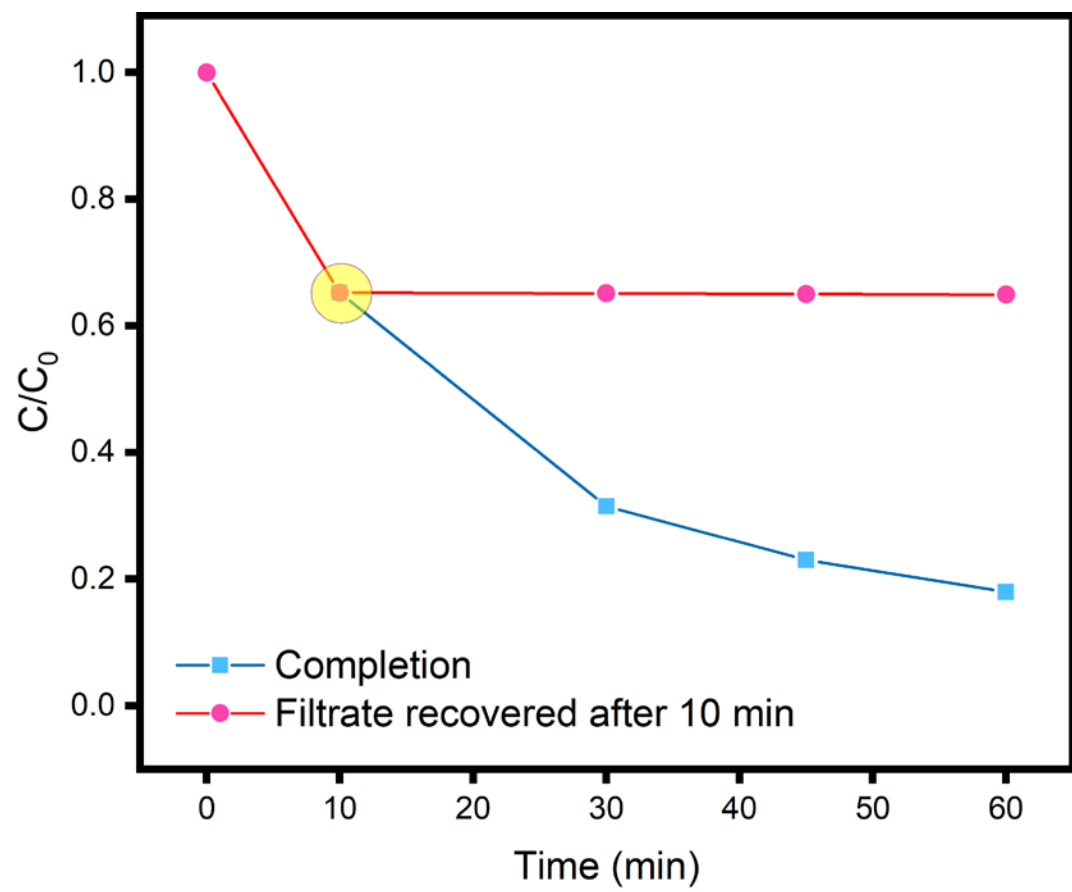


Figure S8: Hot filtration test of $\text{TiO}_2/\text{CQDs}/\text{CdIn}_2\text{S}_4$.

1. Li, X.; Kang, B.; Dong, F.; Zhang, Z.; Luo, X.; Han, L.; Huang, J.; Feng, Z.; Chen, Z.; Xu, J.; et al. Enhanced photocatalytic degradation and H₂/H₂O₂ production performance of S-pCN/WO_{2.72} S-scheme heterojunction with appropriate surface oxygen vacancies. *Nano Energy* **2021**, *81*, 105671, doi:10.1016/j.nanoen.2020.105671.
2. Li, Y.; Wang, K.; Huang, D.; Li, L.; Tao, J.; Ghany, N.A.A.; Jiang, F. Cd_xZn_{1-x}S/Sb₂Se₃ thin film photocathode for efficient solar water splitting. *Applied Catalysis B: Environmental* **2021**, *286*, doi:10.1016/j.apcatb.2020.119872.